Final Report to the
National Earthquake Hazard Reduction Program
U. S. Geological Survey Award Number 07HQGR0022

Title: Joint Seismic Tomography/Location Inversion in the Reno/Carson City Area

Principal Investigators: Leiph Preston and David von Seggern
Nevada Seismological Laboratory
College of Science
U. Nevada - Reno
(lpresto@sandia.gov,vonseg@seismo.unr.edu)

ABSTRACT

We have produced a three-dimensional P velocity and Vp/Vs model of the Reno-Carson City-Tahoe region. We jointly inverted double difference and absolute travel times from over 10,000 local earthquakes for velocity structure and hypocentral locations providing well constrained absolute and relative locations for these events. Results are broadly consistent with the limited 2-D profiles within the study region. Low P velocities and high Vp/Vs are found at shallow depths under the western Nevada basins; however, the vertical resolution within the shallowest 3 km do not allow precise control of basin depths. High velocities and slightly low Vp/Vs predominate the upper crust west of the Sierra crest while generally lower velocities are imaged east of the crest. The deep Tahoe sequence provides a localized but well-imaged view of the lower crust in the hypocentral region, indicating generally upper 6 to low 7 km/s velocities and Vp/Vs at or marginally below a poisson solid. Several small, but well-defined, clusters of earthquakes are delineated in the model. This model provides necessary local-regional scale structural information that can easily be incorporated into the community velocity model of the region. Scenario modeling of probable events whose ray paths to Reno or Carson City sample the upper to mid crust will be improved. Additionally, the revised precision locations point to areas that may need further study and the model provides essential information on the crustal structure of an important tectonic boundary, the SierraNevada Great Basin Boundary Zone.

Introduction

Currently no detailed velocity model exists for the Reno/Carson City urban corridor. Existing "models" are generally at the 10's of km resolution interval, with only sparse points and lines providing more detailed resolution (Louie et al., 2004); as such they cannot provide the required input for 3-D modeling exercises (Pancha et al., 2004) important to earthquake hazard evaluation in this area. Also the current NSL (Nevada Seismological Laboratory) seismic catalog is an unrefined catalog consisting essentially of preliminary locations made in routine operations. These locations, similar to many such catalogs, are inadequate for detailed fault characterization and seismicity interpretations related to fault geometry in a regional tectonic framework. This study jointly rectifies both inadequacies with a combined inversion for velocity and hypocenters.

This study produces the first detailed upper-crustal to mid-crustal velocity model for the urban region of Reno-Sparks-Carson City-Minden/Gardnerville-Lake Tahoe (population ~ 400,000) and serves as the baseline for the development of this area's CVM (Community Velocity Model). A 3-D volume in the rectangular area 38.5N to 40.0N and 121.0W to 119.0W to a depth of roughly 20 km is imaged. This study jointly inverts the NSL seismicity catalog data in the Reno/ Carson City region, thereby obtaining the best-fit velocity model to mid-crustal depths along with best-fit hypocenters. By including the hypocenters in the inversion and by using differential cross-correlation times and differential catalog times in the inversion, it also results in greatly improved hypocenters for the modern (post-1990) NSL seismic catalog, enabling a clearer interpretation of seismic zones and of fault geometry in three dimensions.

An understanding of regional faults and of the 3-D structure of the region including basin geometries is important to accurately quantify regional seismic hazards. Precise hypocentral locations delineate fault zones which will help clarify our understanding of the active fault zones and may even indicate previously unknown faults that should be studied further. Knowing the geometries of fault zones will also aid ground motion studies by providing more accurate descriptions of the source zones for more reliable ground-motion predictions. The 3-D P-wave and S-wave velocity models fill an important gap in our understanding of the geophysical structure of the region since no detailed prior 3-D images of the region exist. The structural images not only are important for correct predictions of ground motions from local faults but also provide important constraints for geophysical and tectonic models of the region, including the Sierra Nevada-Great Basin transition zone. It is possible for structural images to reveal lineaments which have little or no associated seismicity and thus may indicate unknown fault zones that should be the focus for future research into their seismogenic potential.

Preparation of the Catalog Earthquake Time Data

For purposes explained below, largely related to digital data quality, we choose to use the NSL catalog of events from 1990-2006. The area of study was set to be 38.5N to 40.0N and 121.0W to 119.0W (**Figure 1**). No depth or magnitude cutoffs were applied. The original retrieval of catalog data yielded nearly 15,000 earthquakes for this area. After comparing events chronologically, 23 duplicate events were eliminated. All events showing M > 4.0 were checked for correct magnitudes. A total of 48 events had no magnitude, and their magnitudes were

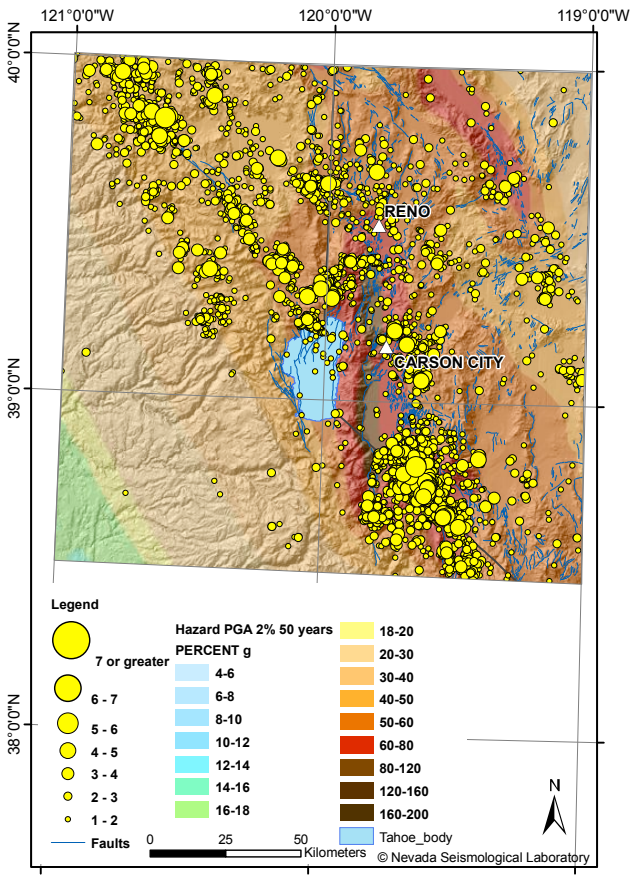

Figure 1: Map of study area with epicenters of NSL catalog earthquakes (1990 -2006) used in the study.

arbitrarily set to 1.0. Doing so for such a small number of events does not affect this study in any significant way. The final catalog for this study comprised 14,775 earthquakes distributed as shown in figure 1. A separate map of the stations which contributed data to this study is shown in figure 2. Figure 3 shows the recurrence curve of the events, and figure 4 shows the initial depth distribution of the events.

Note that in late 2003 to early 2004, an interesting sequence of relatively deep (~ 25-30 km) earthquakes occurred beneath the north end of Lake Tahoe. This sequence was reported in Smith et al. (2004), and it was concluded there that they were associated with a magma intrusion in the lower crust. This set of over 1000 earthquakes are the only ones found (reliably) at depths greater than 20 km in the NSL catalog and form a unique set within the inversion framework. The inversion results will show the influence of these relatively deep events.

Phase arrival times for the earthquakes in the final catalog were all available online. These phase times were all picked by seismic analysts. The normal location process for local events at NSL results in rejection of phase times with high residuals (roughly 0.3 s or larger), but there was no exact prescribed cutoff. As many arrivals are emergent, this helped to ensure that only good arrivals are used and that picked times could be used confidently in windowing waveforms for obtaining cross-correlation times in this study. The phase arrival times were assembled into a dataset suitable for input to the combined tomography/location inversion program. Some data culling was done prior to use in that program. To obtain high-quality, precision hypocentral locations, we required each event to have at least 10 picks and an azimuthal gap no larger than 270°; these criteria were maintained during the inversion.

The distribution of P and S travel-time residuals for the data selected from the final catalog are shown in figure 5. The spread of the data in both cases is truncated by the tendency to not use picks with high residuals in routine location. The standard deviations of the P and S residuals are 0.12 s and 0.13 s, respectively. These correspond closely with input standard deviations for

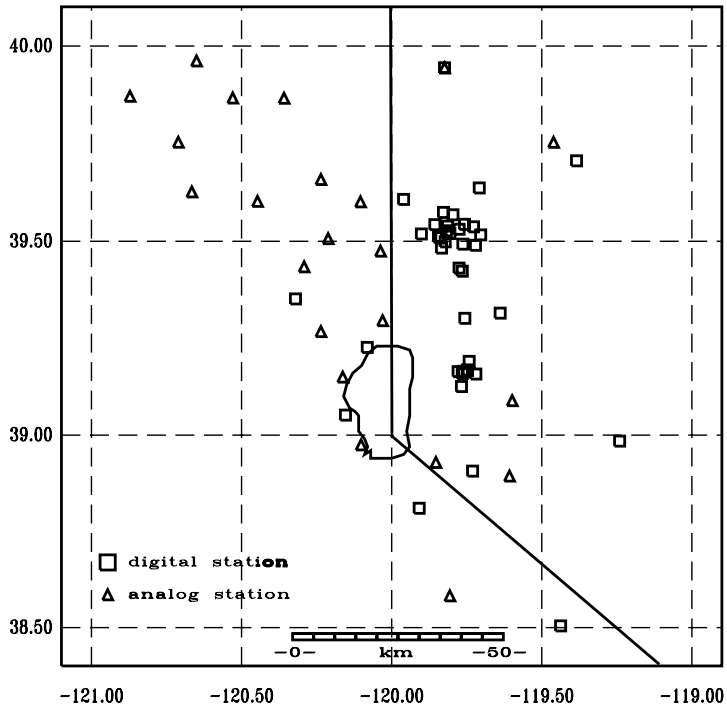

Figure 2: Map of stations which contributed seismic data to this study.

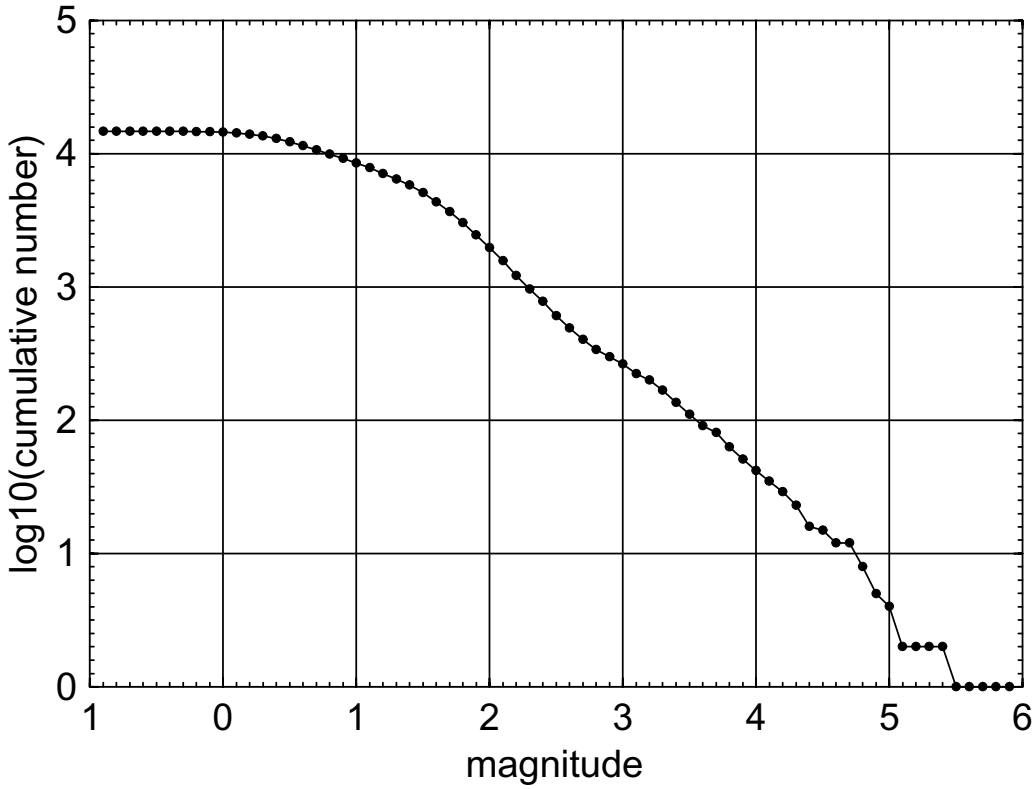

Figure 3: Magnitude distribution of the earthquakes used in this study.

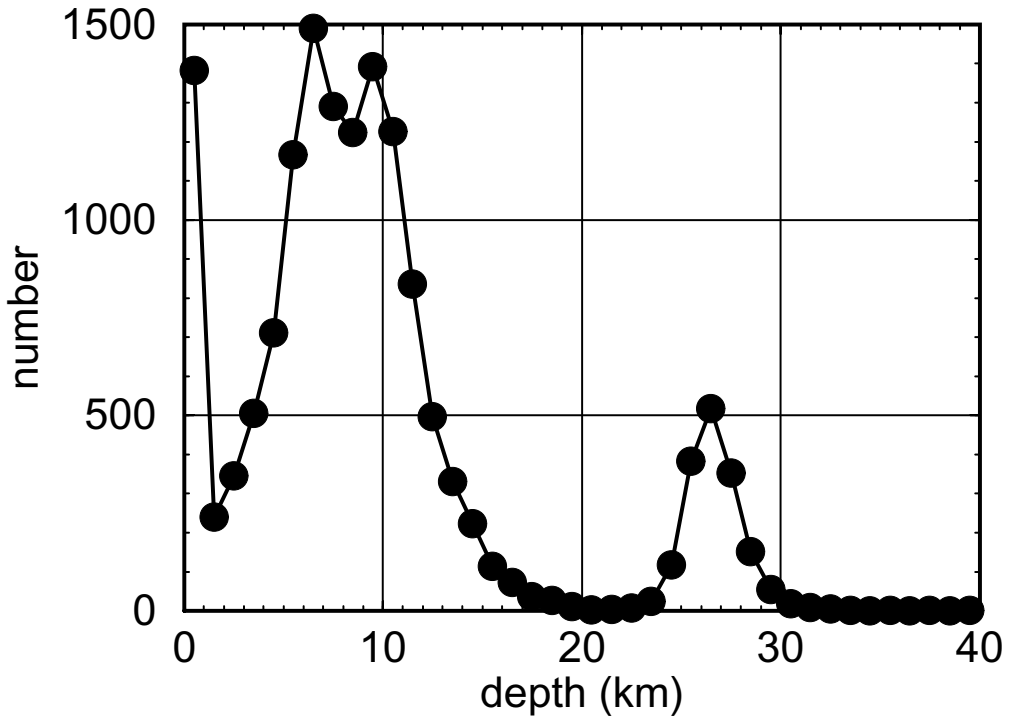

Figure 4: Original catalog depth distribution of earthquakes used in this study.

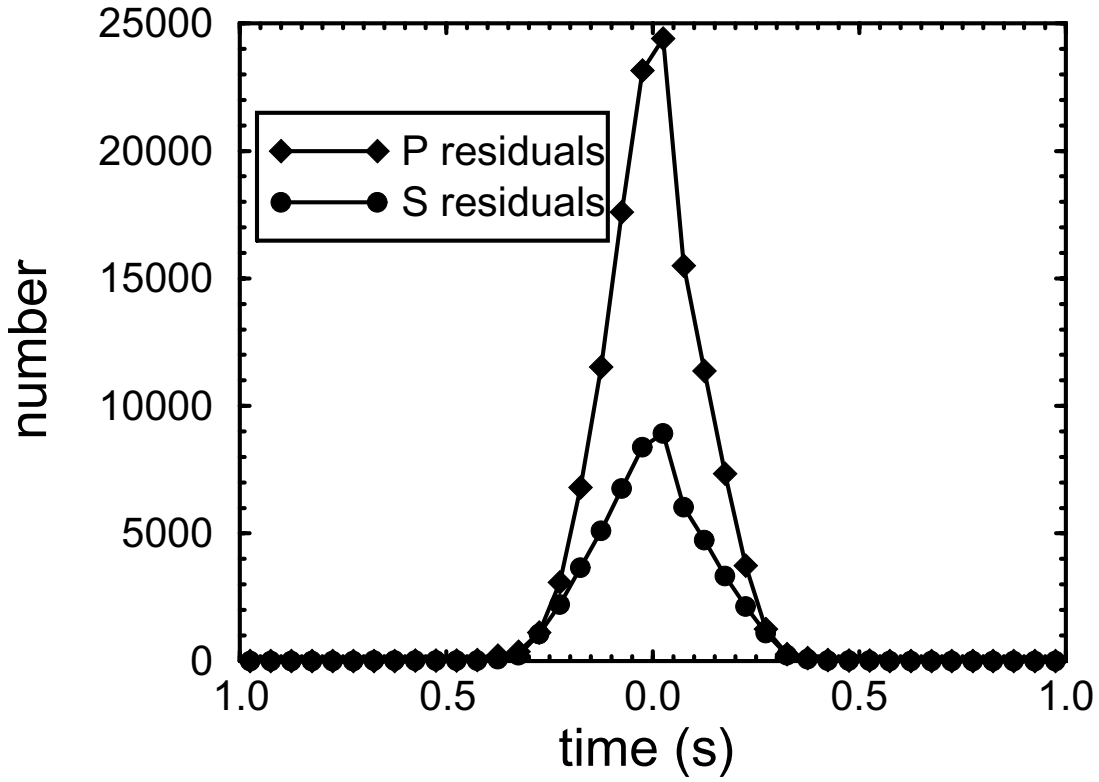

Figure 5: Distributions of catalog P and S travel-time residuals for the earthquakes used in this study.

typical tomography inversions using local earthquake data.

Additional arrival times from explosions were sought from the NSL archives. Events recognized as explosions during routine analysis at NSL are not always well timed; consequently, the arrival times and locations in the archive are not reliable. Due to the distributed spatial character of many of these explosion sources, typically fired at quarry sites, first arrivals are often emergent and difficult to time. We therefore made a magnitude cut of M > 1.5 in accepting explosion data. We also applied a cut to only accept explosions with ≥ 5 P arrivals. This left a set of 23 events (figure 6) which we thought would produce reliable data for inversion. All 23 explosions were retimed and relocated (P waves only) with depth restrained to the topographic surface prior to incorporating their data into the inversion.

Preparation of the Cross-Correlation Time Data

Digital data at high sample rates, typically 100 sps (samples per second), has been recorded at the NSL since the mid-1980's. This type of data, if timing is accurate, has great potential to improve the relative locations of seismic events by cross-correlating signals from nearby events at given stations (Fremont and Malone, 1987; Got et al., 1994; Schaff et al., 2002; Waldhauser

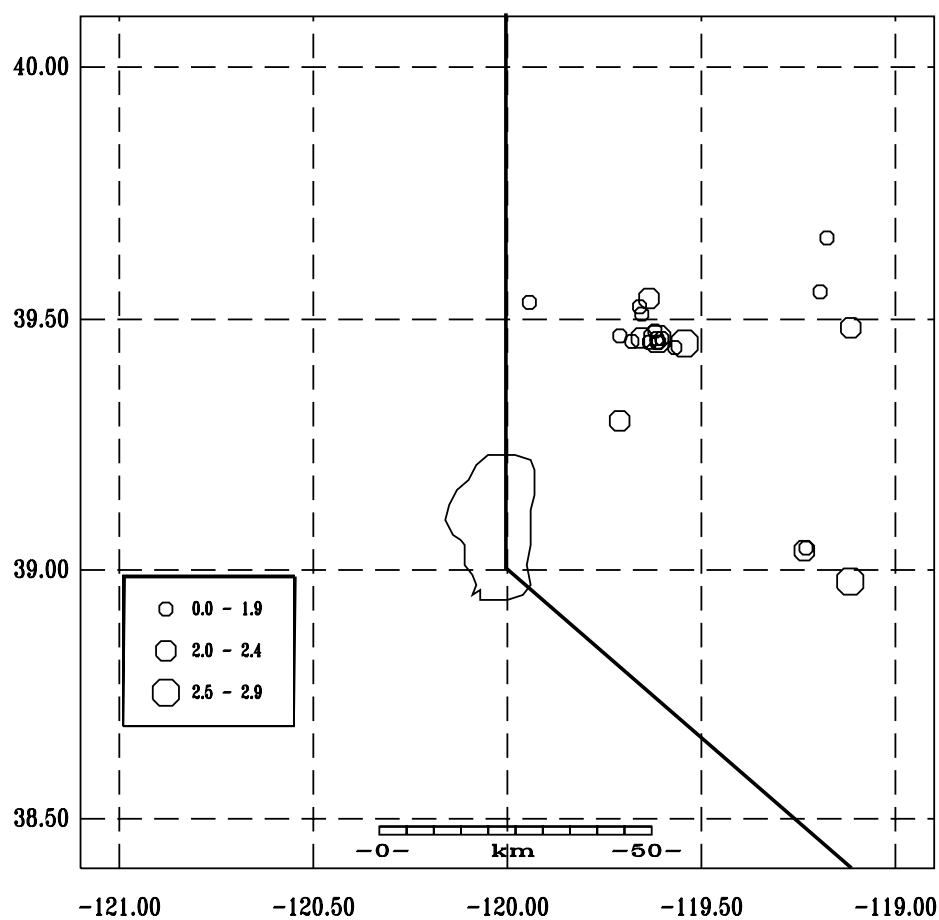

Figure 6: Locations of explosions used in the inversion dataset.

and Ellsworth, 2002; Rowe et al., 2004; Hauksson and Shearer, 2005; Schaff and Waldhauser, 2005). We chose to work with digital data only after the CUSP (CalTech-USGS Seismic Processing) system was installed at the NSL in 1990. Prior digital data was sparse, difficult to retrieve, and often of uncertain time accuracy. Moreover, the NSL catalog prior to 1990, the start of CUSP recording and interactive graphics analysis, had a significantly higher threshold than afterwards. On 01/01/2000, the NSL began to use the Antelope system (BRTT, Inc.) to record and analyze seismic data, and this continues through to present. For purposes of this study, we cut the Antelope data off at the end of 2006. The post-2000, digital data archive was considerably enlarged by the addition of several digital stations in the west-central Nevada and Lake Tahoe regions; consequently, many more earthquakes were located and reported for these regions after 01/01/2000. All digital data arriving at the NSL were sampled at 100 sps and timed in the field under GPS control. The data from all existing analog stations were digitized at NSL on an Earthworm system at 100 sps and incorporated into the Antelope system in real time.

The waveform data for the post-2000 events was readily available online. Timing accuracy of this data is overall excellent. Analog signals are digitized synchronously with the USGS Earthworm digitizer software, and digital signals are time stamped in the field with GPS-controlled recorders. The field data digitizers provide logs of time quality. These have been randomly inspected, and it appears that, for the vast majority of time, the field digitizers were running within accuracies of a few tens of microseconds or less. There was, however, one long time period where approximately 12 digital stations, mostly in northern Nevada within or near the study region, had unreliable time. This occurred from 01/01/2000 to 06/06/2002 due to a switch being incorrectly set in the field acquisition units. This time period for the particular stations involved was tagged so that inaccurate cross-correlation times would not be generated.

The waveform data for the CUSP era of 1990 through the end of 1999 was retrieved, cleaned, and restored to disk in an effort funded by the Yucca Mountain Project. Recovery was not complete, but averaged roughly 90% for the entire ten-year timeframe. An Antelope database (CSS3.0 schema) was created to accommodate the waveforms, thus making the 1990-1999 data appear similar to the 2000-2006 Antelope data. Thereafter, one processing stream essentially handled all the data for cross-correlations. In 2002 a decision was made to down-sample the analog stations from 100 sps to 50 sps for reasons of conserving electronic storage space and of decreasing analysis time. Our cross-correlation processing transparently handles a mix of older 100-sps and newer 50-sps data. Cross-correlation time accuracy is of course reduced by a factor of two if one or both of the signals are recorded at 50 sps rather than 100 sps.

Cross-correlation of waveforms was performed in the time domain. Timing accuracy above the sample interval of the data (0.01 s or 0.02 s) was obtained by fitting a quadratic form to three points of the cross-correlation function, centered on its maximum, and then interpolating a new maximum to the nearest millisecond based on the quadratic fit. Thereby, relative time between event arrivals at a station was determined to as little as one to two milliseconds.

A systematic approach was necessarily taken to limit the amount of cross-correlation data. Because waveform data correlation is known to decrease rapidly with inter-event spacing, there is no benefit in cross-correlating waveforms between events that are a substantial distance apart. For California data, Schaff and Waldhauser (2005) suggest this inter-event distance is on the order of 5 km apart. The problem in applying this criterion is that the catalog locations, which are the only available guide to data selection at the start, are often poor and may be significantly distant from the unknown, true locations. One cannot circumvent this problem; and so we accepted catalog locations to determine inter-event distances, and we selected event pairs which were no more than 5 km apart horizontally and 15 km apart vertically. The vertical distance was set at a rather large tolerance because of the known inability to sometimes accurately determine event depth with local and regional networks. Another criterion which was applied is a limit on the number of events with which a particular event could be paired; this limit was set at 20. This criterion was imposed on the presumption that little improvement in location is obtained past a certain number of links to other events. The first 20 linking events were selected only after sorting the inter-event distances in order to ensure that the ones selected would be the nearest ones.

After all event pairs were selected with the above criteria, waveforms were retrieved and cross-correlated at stations which observed both events in the pair. The result of the cross-correlation is an arrival time difference d(AT) in seconds between events as seen by a particular station. The program also computes d(OT) from the catalog origin times. Both P and S correlation times were computed, depending on what phase arrivals were available from the catalog. Of the millions of computed correlation times, only those times that were associated with an absolute value of cross-correlation coefficient peak ≥ 0.7 were retained. Visual scanning of thousands of cross-correlation functions and earlier work with cross-correlation data statistics show that data with lesser values for the Nevada region are generally not reliable. After this culling, the number of cross-correlation times was over 350,000. One additional culling criterion was applied: the difference $|d(AT) - d(OT)|$ for P or S at a station should be within a tolerance. This tolerance was set at 0.50 s for P and 0.86 s for S (Poisson's ratio multiplier) to eliminate any grossly wrong correlation times even though the correlation coefficient was within tolerance. This last culling only eliminated roughly 1% of the cross-correlation times. Finally, for incorporation into the tomographic inversion, each differential time pick had to be linked to an absolute time pick. This ensures that each event will have both optimal absolute and relative locations.

Tomographic Inversion

We used the inversion procedure of Preston et al. (2007), with some additional features. These include the ability to utilize both P and S travel times and differential times from cross-correlations. Three-dimensional P-velocity and Vp/Vs maps are produced from the inversion in addition to absolutely and relatively relocated seismicity. The inversion is an iterative, non-linear procedure that utilizes full 3-D ray tracing derived from 3-D finite-difference travel times (Vidale, 1990; Hole, 1989). Topographic constraints are strongly enforced so that no rays or earthquakes can wander above the surface in this region of high relief. The extent of the modeled region is from 121° to 119° W longitude, 38.5° to 40° N latitude, and -5 to 37 km depth

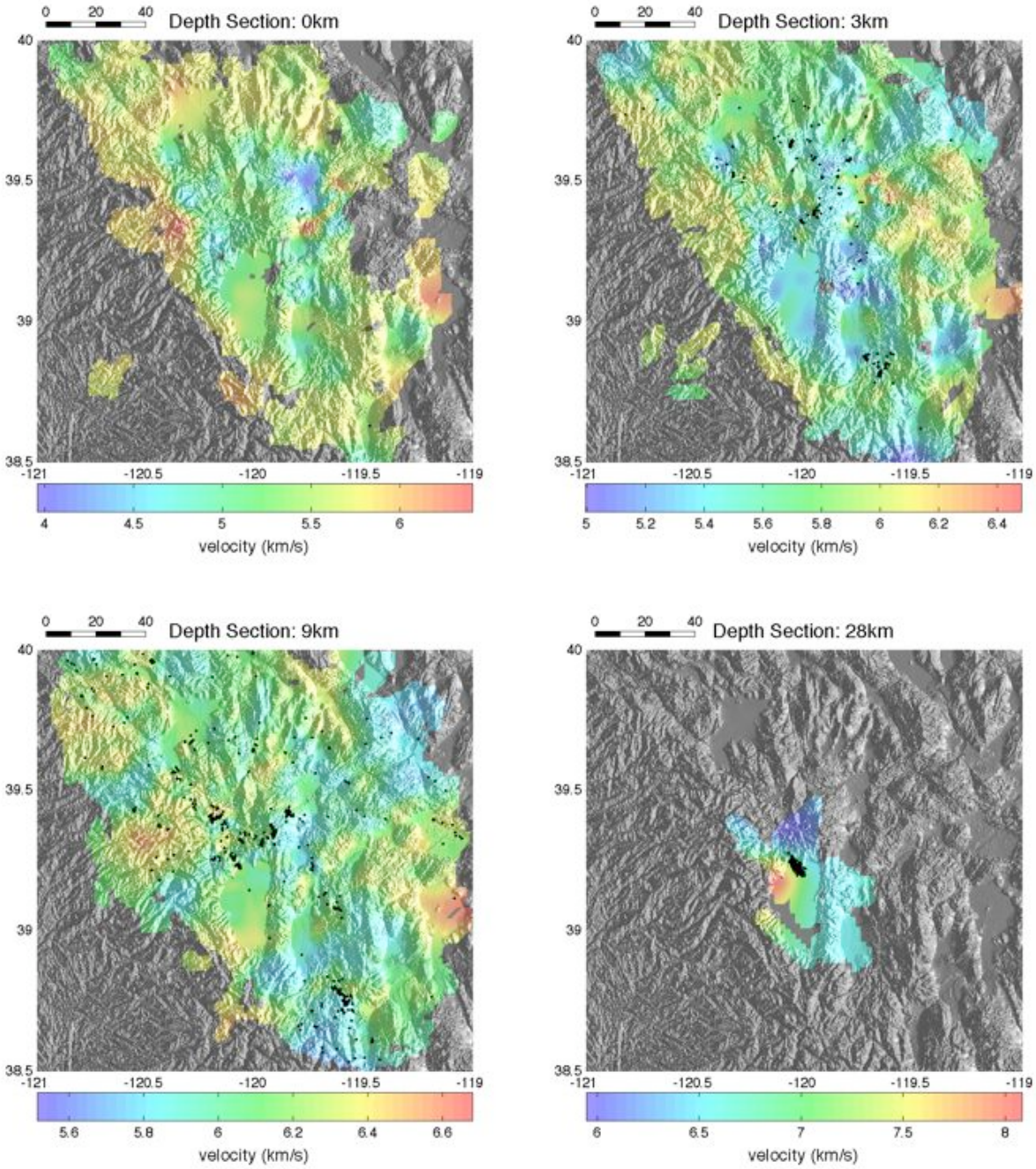

Figure 7: Vp depth sections over shaded relief. Grey regions indicate no ray coverage. Black dots are relocated seismicity within ±1 km of the given depth section.

(relative to sea level). Grid spacing is 2 km horizontally and 1 km vertically. The initial model consisted of catalog earthquake locations and a smoothed version of the standard 1-D model used by NSL to locate events. During inversion, the residuals are screened for outliers, and such are removed. Starting RMS residuals for the culled dataset were 0.15 s for P and 0.18 s for S. Following inversion, the final RMS travel time residuals were 0.05 s for P and 0.11 s for S. Depth and cross-sections through the Vp and Vp/Vs model are shown in figures 7-9.

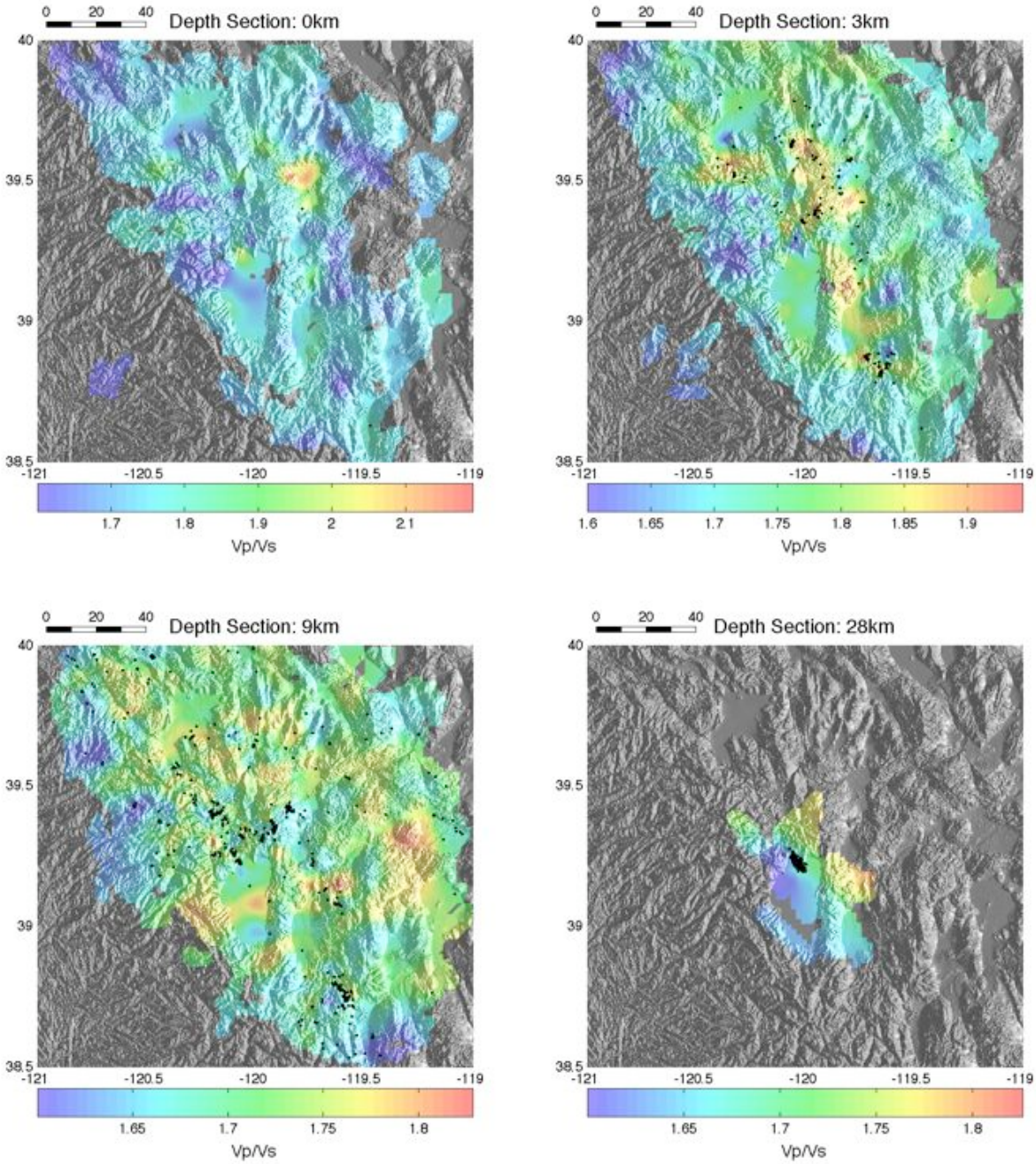

Figure 8: Vp/Vs depth sections over shaded relief. Grey regions indicate no ray coverage. Black dots are relocated seismicity within ±1 km of the given depth section.

Resolution and Error Analysis

The resolution of the final images are assessed using checkerboard tests. In these tests, we perturb the final 3-D model by adding a ±5% repeating pattern that resembles a checkerboard. Rays are then traced through this perturbed model, and noise with the same distribution as the true observations is added to these times to derive a new set of "observations." These are then inverted and the final 3-D model is subtracted from the results to present the recovered pattern of

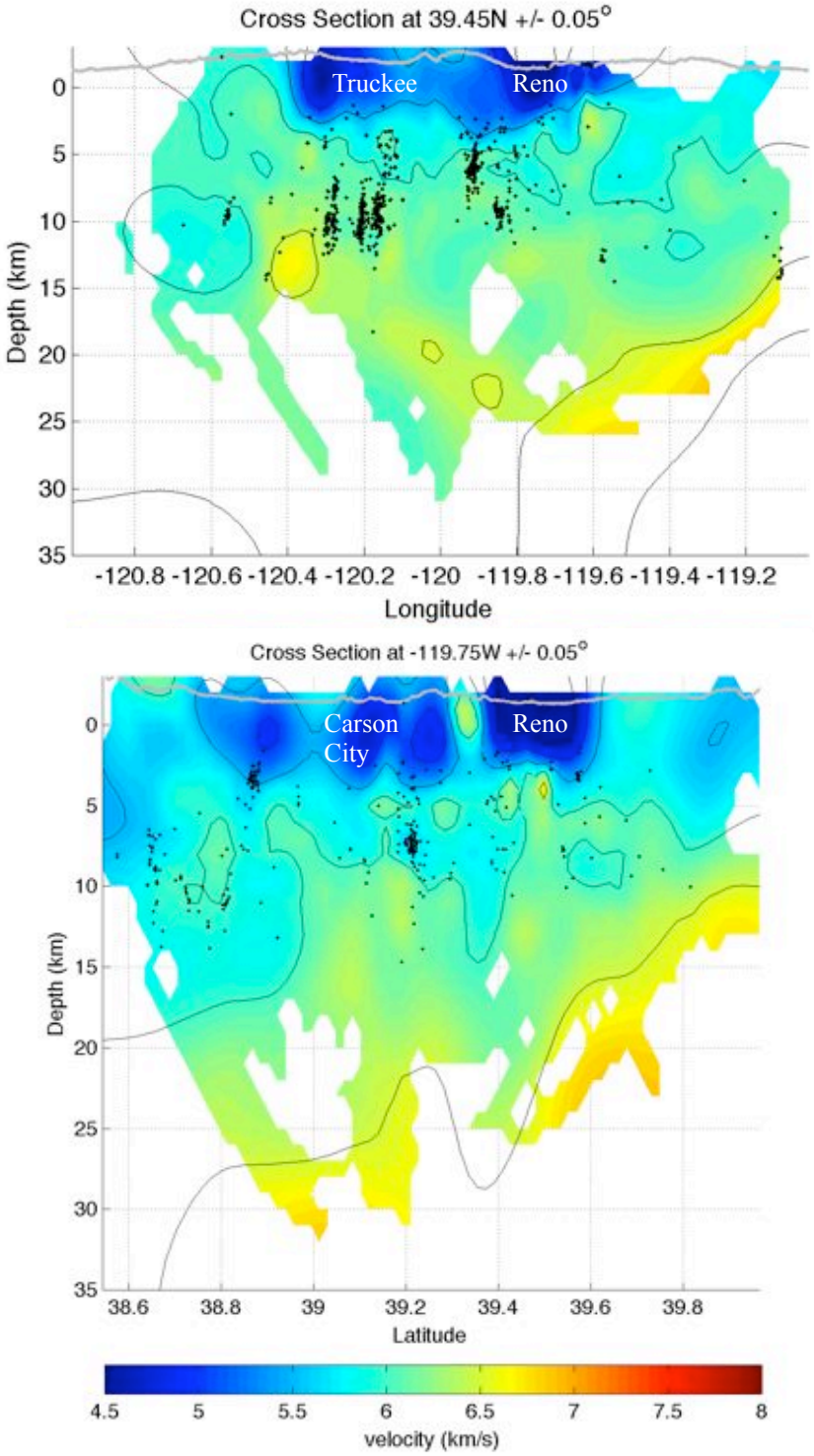

Figure 9: E-W and N-S Vp cross-sections. Black dots are relocated seismicity. Contours are drawn every 0.5 km/s. Grey line is the topography. White areas are those unsampled by rays. VE = 3.

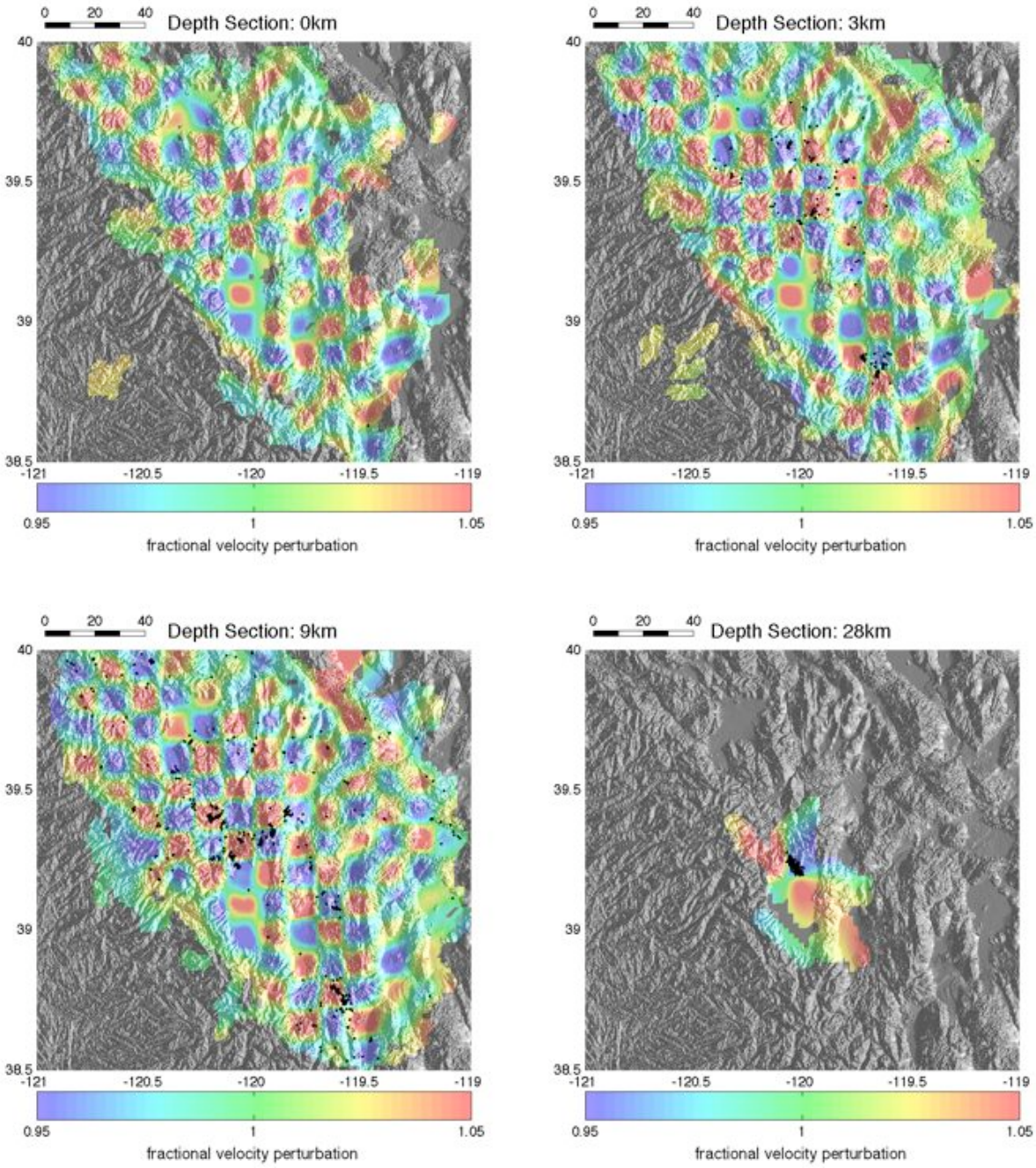

Figure 10: Vp checkerboard resolution test depth sections over shaded relief. Grey regions indicate no ray coverage. Black dots are relocated seismicity within ±1 km of the given depth section. Depth sections 0, 3 and 9 km use 12 km blocks whereas the 28 km depth uses 24 km blocks.

perturbations. Ideally, the recovered pattern will resemble a checkerboard with alternating blocks of lower and higher perturbations. We tested several different resolutions by using different size blocks. For the P-wave model, we used 6, 12 and 24 km blocks for the horizontal dimensions and 4 km for the vertical. The Vp/Vs model utilized 12, 18 and 24 km horizontal by 4 km vertical blocks. The results of the checkerboard tests are shown for selected depth and cross-sections in figures 10-12. Overall resolution at all tested scales is good to very good with recovery of both the pattern and their amplitudes from the high Sierra crest in the west to just

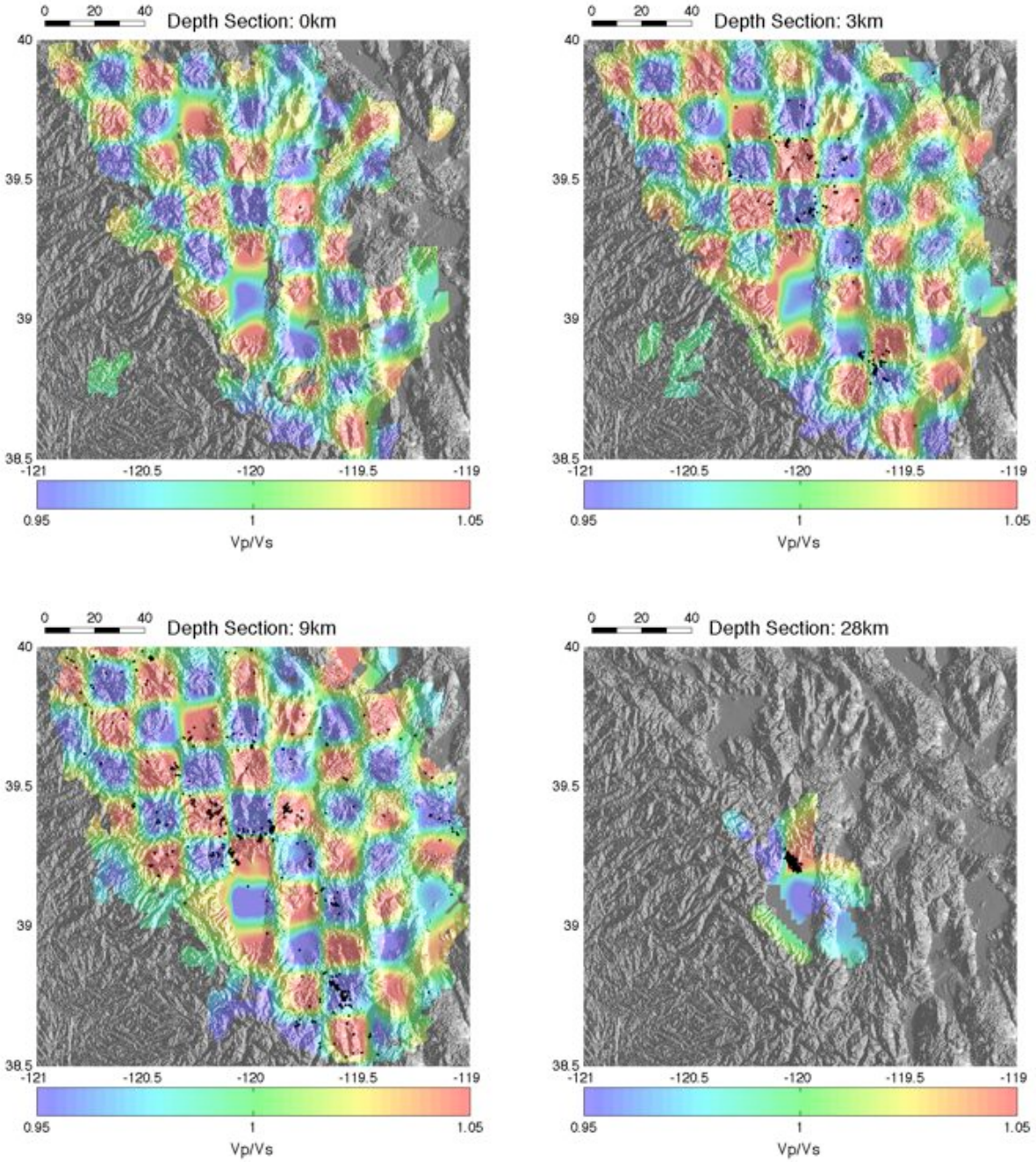

Figure 11: Vp/Vs checkerboard resolution test depth sections over shaded relief. Grey regions indicate no ray coverage. Black dots are relocated seismicity within ±1 km of the given depth section. Depth sections 0, 3 and 9 km use 18 km blocks whereas the 28 km depth uses 24 km blocks.

east of the metropolitan areas of Reno and Carson City, from just north of Reno to south of Carson City, and from ~3-10 km depth. Deeper than ~10 km, resolution degrades to the point that only the volume directly above the deep Tahoe swarm is well-resolved and only at larger scales. Within the deep swarm, resolution is locally excellent where the edges of the blocks are sharply defined; however, resolution rapidly degrades radially away from the deep swarm. Notably, the velocities local to the deep swarm are well resolved as well as a general overall

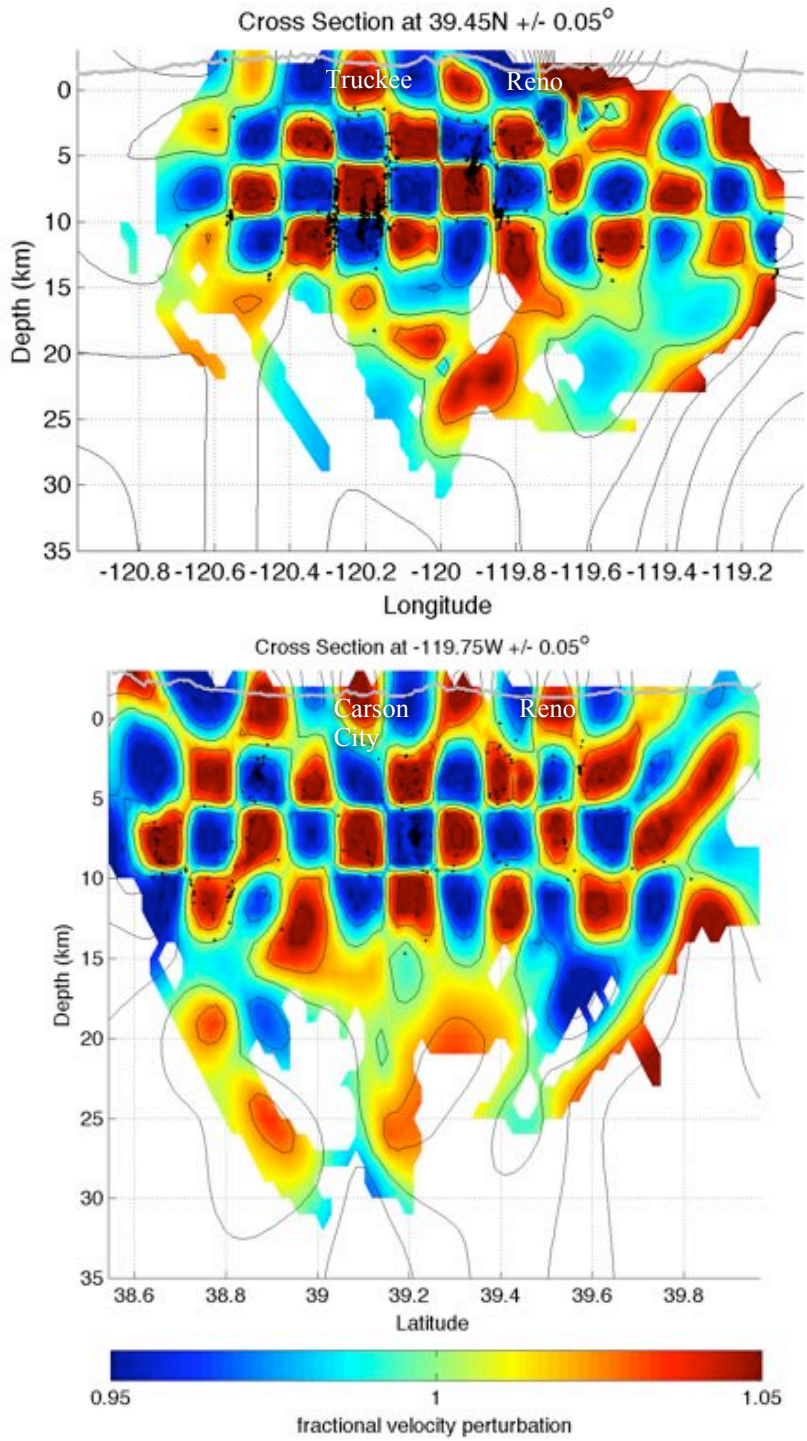

Figure 12: Vp cross-section checkerboard tests with 12 km horizontal by 4 km vertical blocks. Black dots are relocated earthquakes. Countours are drawn at 2.5% intervals. White areas are unsampled by rays. VE = 3.

gradient in velocity, but the P-velocities near 8 km/s and near 6.0 km/s seen in figure 10 are not reliable. We believe these are artifacts from continuation of the local velocity gradient in the swarm to those regions outside that have very limited ray coverage. Shallower than ~3 km depth, resolution, especially in the vertical dimension, is much reduced due to the lack of sources within this depth range. Horizontal resolution at these shallow depths is also relatively poor except in localized areas where station density is high, such as in the urban corridor between Reno and Carson City.

Discussion

We have produced a P-velocity and Vp/Vs model of the Reno-Carson City-Tahoe region. There are several features of interest that are imaged by these models. Although the shallowest 3 km are generally poorly resolved, especially vertically, we do see some correlations with known structures. Notably, the Reno basin is well imaged showing P-velocities near 4.5 km/s at -1 km depth and Vp/Vs greater than 2.0 over much of the basin (figures 7-9). Washoe Valley and Eagle Valley are also resolved at these shallow depths. A high velocity spot, well resolved due to the density of stations near this area, is imaged between Reno and Washoe Valley and is coincident with the Steamboat Hills hydrothermal area (figure 7). High velocities dominate the mostly volcanic mountains east of Reno. Subdued velocities (Vp<6 km/s) are the rule in a broad region from Reno to Carson Valley in the east and bounded by the high Sierra Crest to the west (figures 7 and 9). This region is broadly coincident with the highest rates of seismicity at depth and with high post-Miocene deformation associated with the Sierra Nevada to Basin and Range transition zone (Schweickert et al., 2000). North of the latitude of Reno, resolution degrades except under Antelope Valley where resolution remains fair. Unfortunately, the depth extent of the basins under Reno and Carson City are not resolved by our model primarily due to the lack of sources within the critical depth range. Higher resolution seismic data, most likely in the form of active sources, would be necessary to address in more detail the seismic velocity and depth extent of the urban basins.

Within 3-km depth we begin to see the shallowest locations of seismicity (figure 7). Due to the use of cross-correlation travel times, we can image lineaments of seismicity, in a relative sense, very accurately. Notable at this shallow depth is part of the Double Springs Flat aftershock sequence of 1995 just southeast of Carson Valley. Most of the seismicity within the cluster lies along a north-to-northeast-striking lineament under the Pine Nut Mountains. Smaller clusters of events are also imaged just north of Lake Tahoe under Mount Rose, just east of the Sierra Crest; and there are a few scattered events northwest of Reno and between Washoe Valley and Carson City. Velocities at this depth show the same broad-scale trend as closer to the surface with low velocities dominating the region between the Sierra crest and the mountains east of Reno and high velocities from the Sierra crest westward. Vp/Vs at this depth generally is at or slightly lower than a Poisson solid, with a few elevated areas that may be of questionable resolvability except for the larger regions or where the seismicity is dense. A N-S band of higher Vp/Vs lies along the Sierra front range mountains that lie just west of the urban corridor. Also, a prominent region of high Vp/Vs lies just to the south of Antelope Valley. Low Vp/Vs comprise a bulk of the Sierra west of the Sierra crest.

The majority of seismicity occurs within the depth range from 4-10 km. Seismogenically, the patterns apparent at 3 km continue down to roughly 7 km depth, notably the Double Springs Flat aftershock sequence, a few clusters of events north of Lake Tahoe continuing north under Truckee to northwest of Antelope Valley, a group of events northwest of Reno, and a small cluster between Washoe Valley and Carson City. There is apparently a hole in seismicity between Reno and Truckee, and seismicity west of the Sierra crest is weak to non-existent. The two most prominent clusters between 3 and 7 km depth are the Double Springs Flat sequence and a tight cluster of events near Mount Rose, which appears to be centered at ~6 km depth. Below 7 km, the seismicity pattern changes. The Double Springs Flat sequence continues, but is diminishing with depth. Seismicity from Truckee northwestward into Antelope Valley continues but becomes more diffuse. The tight cluster near Mount Rose disappears and is replaced by a northeast-trending zone that trends toward a vertical lineament of seismicity that overlies the deep Tahoe sequence. We have termed this vertical lineament of seismicity the "shallow Tahoe sequence". This sequence is spatially and temporally correlated with the deep Tahoe sequence (discussion follows) that occurred in 2003-2004 (Smith et al., 2004). We have carefully investigated the depths of the shallow sequence, and the vertically extensive lineament is supported by the travel times. Von Seggern et al. (2008) interpret this structure as due to volatiles migrating upward from the deep Tahoe intrusion and producing earthquakes in the more brittle upper crust. The cluster of events between Washoe Valley and Carson City ceases by 8 km, but a NNW-striking lineament of seismicity just east of Carson City appears between 8 and 11 km depth. P velocities increase slightly on average, with average velocities just below 6 km/s at 4 km tending toward just above 6 km/s by 10 km depth. Within this depth range, correlations with surface features fade into a weak pattern of northeast-striking bands of slightly higher and lower velocity. Vp/Vs generally becomes smoother with depth, with an average very near a Poisson solid. High Vp/Vs regions imaged at shallow depths (3-7 km) fade away by 6 km depth, but a prominent high Vp/Vs appears by 8-km depth under the mountains east of Reno and the general structure mimics the weak NE-striking banding of the P velocities. There may be a slight hint of lower than average Vp/Vs west of the Sierra crest; this may be indicative of a depth-persistent highly silicic material.

From 11 to 20 km depth, seismicity falls off rapidly with depth. The shallow Tahoe sequence persists to 14 km depth, with the last of the Double Springs Flat events occurring down to this depth as well. Two additional tight clusters of events occur in this depth range, both in the northwest part of the model. One occurs at 14-km depth west of Yuba Pass, while the other occurs more as a northwest-striking lineament northwest of Antelope Valley between 15 and 17 km depth. From 17 km to the top of the deep Tahoe sequence, no events occur. The resolution of the Vp model degrades below the depth of the main group of events at 12 km except directly above the deep Tahoe sequence and near the cluster northwest of Antelope Valley. In a general sense, velocities increase from the low 6 km/s range to the upper 6 km/s range. Vp/Vs resolution also degrades below 12 km, but generally indicates nearly constant Vp/Vs very near the value of a Poisson solid. We need to note that the area of high Vp/Vs directly above the deep Tahoe sequence centered under the north end of Lake Tahoe may not be real. Error analysis indicates

this region has a high estimated standard error and there is no clear evidence of a high Vp/Vs region based on S-wave travel times through this region.

The deep Tahoe sequence dominates the depths from 21 to 34 km depth with the vast majority occurring within the range 25 - 30 km depth centered under the northwestern corner of Lake Tahoe. The cluster is especially well defined horizontally where it forms a northwest-southeast striking structure that dips steeply to the northeast. These results are consistent with analyses done in Smith et al. (2004), where it was concluded, based on combined seismic and geodetic observations, that these events were caused by a volcanic intrusion which opened a 1-m crack. Velocities within this depth range are only well resolved in the vicinity of the seismicity. However, Vp very near the seismicity is imaged as very slow for this depth, in the lower 6 km/s range. Vp/Vs appears to be at or above a Poisson solid value in the shallow portions of the sequence trending to lower Vp/Vs deeper. It is important to note that, due to the paucity of crossing ray paths at this depth, the inherent trade-off between absolute depth of the events and the velocities is particularly problematical.

Conclusion

We have produced a 3-D velocity model that will be important as a background model for scenario earthquake modeling within the Reno-Carson City-Tahoe region. Our results are consistent with the 2-D refraction-derived model of Louie et al. (2004) where the models overlap. This local-regional scale model will be especially important for accurate and realistic modeling of events that will sample the upper crust such as from the southern leg of the Genoa Fault to Reno. Higher resolution data based on gravity, geological evidence, and other seismological techniques will allow basin resolution where necessary and as data availability permit. Besides the addition of upper-crustal information for modeling purposes, our modeling effort also provides a clearer picture of where we should focus future studies and scenario modeling. Seismicity bands such as those imaged near Carson City, Mount Rose, and from Truckee to northwest of Antelope Valley suggest these may be areas where more study should be focused in addition to those studies already addressing the well-known hazards in the area imaged here. Additionally, the velocity images constrain any 3-D model of the Sierra Nevada-Great Basin Boundary Zone, an important tectonic boundary.

References

Fremont, M.-J., and S. D. Malone, High precision relative locations of earthquakes at Mount St. Helens, Washington, *J. Geophys. Res*. 93, 10,223-10,236, 1987.

Got, J.-L., J. Frechet, and F. W. Klein, Deep fault plane geometry inferred from multiplet relative relocation beneath the south flank of Kilauea, *J. Geophys. Res*., 99, 15,375-15,386, 1994.

Haukson, E., and P. Shearer, Southern California hypocenter relocation with waveform cross-correlation, Part 1: Results using double-difference method, *Bull. Seimol. Soc. Am.*, 95, 896-903, 2005.

Hole, J.A. and B.C. Zelt, Three-dimensional finite-difference reflection travel times, *Geophys. J. Int.*, 121, 427-434, 1995.

Louie, J.N, W. Thelen, S.B. Smith, J.B. Scott, M. Clark, and S. Pullammanappallil, The northern Walker Lane refraction experiment: Pn arrivals and the northern Sierra Nevada root, *Tectonophysics*, 388, 253-269, 2004.

Pancha, A., J.G. Anderson, J.N. Louie, and A. Anooshehpoor, Data and simulation of ground motion for Reno, Nevada, 13th World Conference on Earthquake Engineering, Vancouver, B.C., Canada, Aug. 1-6, 2004, Paper No. 3452, 2004.

Preston, L., K. Smith, and D. von Seggern, P wave velocity structure in the Yucca Mountain, Nevada, region, *J. Geophys. Res.*, 112, B11305, doi:10.1029/2007JB005005, 2007.

Rowe, C.A., C.H. Thurber, and R.A. White, Dome growth behavior at Soufriere Hills Volcano, Montserrat, revealed by relocation of volcanic event swarms, 1995-1996, *J. Volcanol. Geotherm. Res.*, 134, 199-221, 2004.

Schaff, D. P., G. H. R. Bokelmann, and G. C. Beroza, High-resolution image of Calaveras Fault seismicity, *J. Geophys. Res.*, 107, doi:10.1029/2001JB000633, 2002.

Schaff, D.P., and F. Waldhauser, Waveform cross-correlation-based differential travel-time measurements at the northern California seismic network, *Bull. Seismol. Soc. Am.*, 95, 2446-2461, 2005.

Schweickert, R.A., M.M. Lahren, R. Karlin, J. Howle, and K. Smith, Lake Tahoe active faults, landslides, and tsunamis, *in* Largeson, D.R., S.G. Peters, and M.M. Lahren, eds., Great Basin and Sierra Nevada: Boulder, CO, Geol. Soc. Am. Field Guide 2, 1-22, 2000.

Smith, K.D., D. von Seggern, G. Blewitt, L. Preston, J.G. Anderson, B.P. Wernicke, and J.L. Davis, Evidence for deep magma injection beneath Lake Tahoe, Nevada-California, *Science*, 305, 1277-1280, 2004.

Vidale, J.E., Finite-difference calculation of traveltimes in three dimensions, *Geophysics*, 55, 1504-1507, 1990.

von Seggern, D.H., K.D. Smith and L.A. Preston, Seismic spatial-temporal character and effects of a deep (25-30 km) magma intrusion below north Lake Tahoe, California-Nevada, *Bull. Seismol. Soc. Am.*, 98, doi: 10.1785/0120060240, 2008

Waldhauser, F., and W. L. Ellsworth, Fault structure and mechanics of the Hayward Fault, California, from double-difference earthquake locations, *J. Geophys. Res.*, 107, doi: 10.1029/2000JB000084, 2002.